0022-3565/09/3281-69–82$20.00
THE JOURNAL OF PHARMACOLOGY AND EXPERIMENTAL THERAPEUTICS
JPET 328:69–82, 2009

Vol. 328, No. 1
146068/3418014
Printed in U.S.A.

A Single in Vivo Application of Cholinesterase Inhibitors Has Neuron Type-Specific Effects on Nicotinic Receptor Activity in Guinea Pig Hippocampus

Manickavasagom Alkondon, Yasco Aracava, Edna F. R. Pereira, and Edson X. Albuquerque

Department of Pharmacology and Experimental Therapeutics, University of Maryland School of Medicine, Baltimore, Maryland

Received September 12, 2008; accepted October 7, 2008

ABSTRACT

The present study was designed to test the hypothesis that an acute in vivo treatment with reversible or irreversible acetylcholinesterase (AChE) inhibitors modifies the activities of nicotinic receptors (nAChRs) in hippocampal neurons. Here, whole-cell nicotinic responses were recorded from CA1 interneurons in hippocampal slices obtained from male guinea pigs at 1, 7, or 14 days after treatment with the irreversible AChE inhibitor, soman (1× LD_{50} s.c.), and/or the reversible AChE inhibitor, galantamine (8 mg/kg i.m.). Naive animals were used as controls. Three types of nAChR responses, namely types IA, II, and III, which were mediated by $\alpha7$, $\alpha4\beta2$, and $\alpha3\beta2\beta4$ nAChRs, respectively, could be recorded from the interneurons. The magnitude of $\alpha7$ nAChR currents was neuron-type dependent. Stratum radiatum interneurons (SRIs) with thick initial dendrites had the largest $\alpha7$ nAChR currents. Acute challenge with soman caused sustained reduction of type IA current amplitudes recorded from stratum oriens interneurons and increased the ratio of acetylcholine- to choline-evoked current amplitudes recorded from SRIs. In guinea pigs that developed long-lasting convulsions after the soman challenge, there was a sustained reduction of $\alpha3\beta2\beta4$ nAChR responses. Acute treatment with galantamine had no effect on type IA or III responses, whereas it decreased the incidence of type II currents. Pretreatment of the guinea pigs with galantamine prevented the suppressive effect of soman on type III responses. The neuron type-specific changes in nAChR activity induced by soman, some of which could be prevented by galantamine, may contribute to the maintenance of pathological rhythms in the hippocampal neuronal network.

A recent study from our laboratory demonstrated that galantamine effectively and safely counteracts the acute toxicity of organophosphorus (OP) compounds in guinea pigs, the best nonprimate model to predict the effectiveness of antidotes against OP toxicity in humans (Albuquerque et al., 2006; Pereira et al., 2008). A single exposure to the OPs is lethal and is the likely scenario in a terrorist attack or accidental poisoning. Although OP nerve agents and pesticides interact with numerous molecular targets (Albuquerque et al., 1985; Schuh et al., 2002), irreversible inhibition of acetylcholinesterase (AChE), the enzyme that hydrolyzes the neurotransmitter acetylcholine (ACh), appears to be a major determinant of their acute toxicity. The cholinergic syndrome characteristic of OP intoxication results in part from the actions of accumulated ACh on peripheral and central cholinergic receptors. Miosis, hypersecretions, bronchoconstriction, bradycardia, incontinence, and diarrhea result from muscarinic receptor overstimulation. Hyperactivation of nicotinic receptors (nAChRs) triggers muscle fasciculation, whereas their subsequent desensitization leads to muscle weakness. Central nervous system-related effects include anxiety, restlessness, confusion, ataxia, tremors, seizures, and cardiorespiratory paralysis (Newmark, 2007).

Galantamine, a reversible AChE inhibitor currently approved for symptomatic treatment of mild-to-moderate Alzheimer's disease, is also known to act as an allosteric potentiating ligand at various nAChRs (Pereira et al., 1993; Schrattenholz et al., 1996). Some studies have reported that acting primarily as a nicotinic allosteric potentiating ligand

This study was supported by the National Institutes of Health CounterACT Program through the National Institute of Neurological Disorders and Stroke [Award UO1NS059344] and by the Army Research Office [Contract W911NF-06-1-0098].

Patents are pending for the method of prophylactically treating organophosphorus poisoning.

Article, publication date, and citation information can be found at http://jpet.aspetjournals.org.

doi:10.1124/jpet.108.146068.

ABBREVIATIONS: OP, organophosphorus; AChE, acetylcholinesterase; ACh, acetylcholine; nAChR, nicotinic acetylcholine receptor; EPSC, excitatory postsynaptic current; SRI, stratum radiatum interneuron; ACSF, artificial cerebrospinal fluid; QX-314, lidocaine *N*-ethyl bromide; NMDA, *N*-methyl-D-aspartate; SOI, stratum oriens interneuron; SPI, stratum pyramidal interneuron; SO, stratum oriens; SR, stratum radiatum; SLM, stratum lacunosum moleculare; MLA, methyllycaconitine; α-BGT, α-bungarotoxin.

galantamine increases the activity of nAChRs in acute hippocampal slices (Santos et al., 2002). Others have reported that reversible AChE inhibition by galantamine and other compounds causes desensitization of ACh-induced activation of α7 nAChRs while prolonging the action of ACh at non-α7 nAChRs (Fayuk and Yakel, 2004). Very little is known regarding the protracted effects of an acute in vivo treatment with galantamine or challenge with OP compounds on the activity of functional nAChRs in the brain.

The physiological and functional properties of neuronal nAChRs have been studied primarily in the rat and mouse brain (Alkondon et al., 1997, 1999, 2004, 2007b; Jones and Yakel, 1997; Frazier et al., 1998; McQuiston and Madison, 1999; Alkondon and Albuquerque, 2004, 2005). In general, three types of pharmacologically distinct nAChR responses, namely types IA, II, and III, which are mediated by α7, α4β2, and α3β2β4 nAChRs, respectively, have been recorded from interneurons of rat and mouse hippocampi. Both α7 and α4β2 nAChRs are found on the somatodendritic regions of interneurons, and activation of these receptors leads to GABA release onto both pyramidal neurons and interneurons (Alkondon et al., 1999; Alkondon and Albuquerque, 2001). On the other hand, α3β2β4 nAChRs are located on glutamatergic neurons/axons that synapse onto CA1 interneurons; activation of these nAChRs triggers excitatory postsynaptic currents (EPSCs) that can be recorded from CA1 interneurons (Alkondon and Albuquerque, 2005). Although the effects of nAChR ligands on synaptic plasticity and transmission have been demonstrated at the network level (Mann and Greenfield, 2003; Wanaverbecq et al., 2007), the types and prevalence of nAChRs have never been characterized before in guinea pig hippocampal slices at the cellular level.

The present study was designed to identify pharmacologically the nAChR subtypes that subserve nicotinic responses in CA1 interneurons of guinea pig hippocampal slices and to investigate changes in nAChR activity after a single exposure of guinea pigs to soman and/or galantamine. Evidence is provided herein that the pattern of nAChR expression in the hippocampus of guinea pigs is similar to that reported for other rodents, except that α7 nAChR expression in CA1 stratum radiatum interneurons (SRIs) is higher for guinea pigs than age-matched rats. An acute exposure to soman triggered: 1) a transient enhancement of ACh-induced α7 nAChR activation in CA1 SRIs, 2) a long-lasting reduction of the α7 nAChR activity in stratum oriens interneurons (SOIs), and 3) a prolonged suppression of the α3β2β4 nAChR regulation of glutamatergic transmission impinging onto CA1 SRIs. In contrast, the acute in vivo treatment with galantamine had no effect on α7 nAChR activity, albeit it caused a prolonged reduction of the α4β2 nAChR activity in the CA1 SRIs. Pretreatment of the guinea pigs with galantamine counteracted the effects of soman on α3β2β4 nAChRs. As discussed herein, the effects of soman on the activity of the various nAChRs in the hippocampus have the potential to increase feed-forward while decreasing feedback inhibition of CA1 pyramidal neurons. The treatment with galantamine can counteract the imbalance between inhibition and excitation in the animals exposed to soman and, thereby, prevent the development of abnormal neuronal synchronization that would favor the sustainment of epileptiform activity in the hippocampus.

Materials and Methods

Animals. Male Hartley guinea pigs [Crl(HA)Br] that were 9 days old were purchased from Charles River Laboratories, Inc. (Wilmington, MA) and housed for 2 days before the experiments in groups of three to five per cage in a temperature- and light-controlled animal care unit. Handling of the animals was according to the regulations of the Association for Assessment and Accreditation of Laboratory Animal Care, complied with the standards of the Animal Welfare Act, and adhered to the principles of the *Guide for the Care and Use of Laboratory Animals* (Institute of Laboratory Animal Resources, 1996).

Guinea pigs were divided into four experimental groups. The control group consisted of animals not injected with any agents and were used at postnatal days 11 to 12 (referred to as P11), 16 to 19 (referred to as P18), and 22 to 26 (referred to as P25). The soman group consisted of animals (11–12 days old) that received an s.c. injection of 25.2 μg/kg soman (1× LD_{50}) between the shoulder blades. The galantamine group consisted of animals (11–12 days old) that received an i.m. injection of 8 mg/kg galantamine. The galantamine plus soman group consisted of animals (11–12 days old) that were treated with 8 mg/kg galantamine i.m. 30 min before the challenge with 25.2 μg/kg soman s.c. Animals in each group were used at 1, 7, and 14 days after the injections. As listed in Table 1, nearly half of the animals died at 24 h in the soman group, and the animals in all other groups and time points survived.

Hippocampal Slices. Guinea pigs were euthanized by asphyxia in a CO_2 atmosphere followed by decapitation. Their brains were removed, and the hippocampi were dissected out in cold artificial cerebrospinal fluid (ACSF). Hippocampal slices, 300-μm-thick, were cut using a Vibratome sectioning system (Leica VT 1000S; Leica, Nusslock, Germany). Slices were stored at room temperature in ACSF, which was bubbled with 95% O_2/5% CO_2 and composed of 125 mM NaCl, 25 mM $NaHCO_3$, 2.5 mM KCl, 1.25 mM NaH_2PO_4, 2 mM $CaCl_2$, 1 mM $MgCl_2$, and 25 mM glucose. CA1 interneurons in hippocampal slices were visualized by means of infrared-assisted videomicroscopy for patch-clamp recordings. In addition, biocytin labeling was used for postrecording morphological identification of the neurons.

Patch-Clamp Recordings. Live neurons in the hippocampal slices were visualized using the 40× water immersion objective of a Zeiss upright microscope (Carl Zeiss, Oberkochem Germany), and the images were viewed on a monitor using a digital camera. Slices were superfused with ACSF at 2 ml/min at room temperature. The ACSF contained atropine (0.5 μM) to block muscarinic receptors and bicuculline (10 μM) to block $GABA_A$ receptors. EPSCs and agonist-evoked whole-cell currents were recorded from the soma of various neurons according to the standard patch-clamp technique using an EPC9 amplifier and PULSE software (ALA Scientific Instruments, Inc., Westbury, NY). Agonists were applied to the slices via a U tube, and antagonists were applied via the bath perfusion. The internal pipette solution contained 0.5% biocytin in addition to 10 mM ethylene-glycol bis(β-amino-ethyl ether)-*N*-N′-tetraacetic acid, 10 mM HEPES, 130 mM Cs-methane sulfonate, 10 mM CsCl, 2 mM $MgCl_2$, and 5 mM QX-314 (pH adjusted to 7.3 with CsOH; 340 mOsm).

TABLE 1
Survival rate of guinea pigs 24 h after each treatment
Animals surviving 24 h after treatment remained alive during the 2-week time frame used in this study.

Group	No. of Guinea Pigs Used	No. of Guinea Pigs Survived 24 h after Treatment	% Survival at 24 h after Treatment
Control (no injection)	28	28	100
Soman (25.2 μg/kg s.c.)	37	19	51
Galantamine (8 mg/kg i.m.)	16	16	100
Galantamine + soman	12	12	100

Membrane potentials were corrected for liquid junction potential. All experiments were carried out at room temperature (20–22°C).

Data Analysis. The peak amplitude and net charge of nicotinic currents and net charge of NMDA EPSCs were analyzed using the pClamp 9 software (Molecular Devices, Sunnyvale, CA). The data are expressed as mean ± S.E.M., and statistical significance was analyzed using Student's *t* test, Mann-Whitney nonparametric analysis, and Fisher's exact test using the GraphPad InStat program (GraphPad Software Inc., San Diego, CA). Nonparametric linear regression was carried out using the StatsDirect program (StatsDirect Ltd, Cheshire, UK).

Results

Interneurons Studied in the CA1 region of Guinea Pig Hippocampal Slices. In this study, whole-cell patch-clamp recordings were obtained from visually identified interneurons found in three locations in the CA1 field of hippocampal slices (see Fig. 1A). Interneurons were studied in the stratum oriens (referred to as SOIs), near the pyramidal layer (referred to as SPIs), and in the stratum radiatum (referred to as SRIs) (Fig. 1A). Postrecording reconstruction

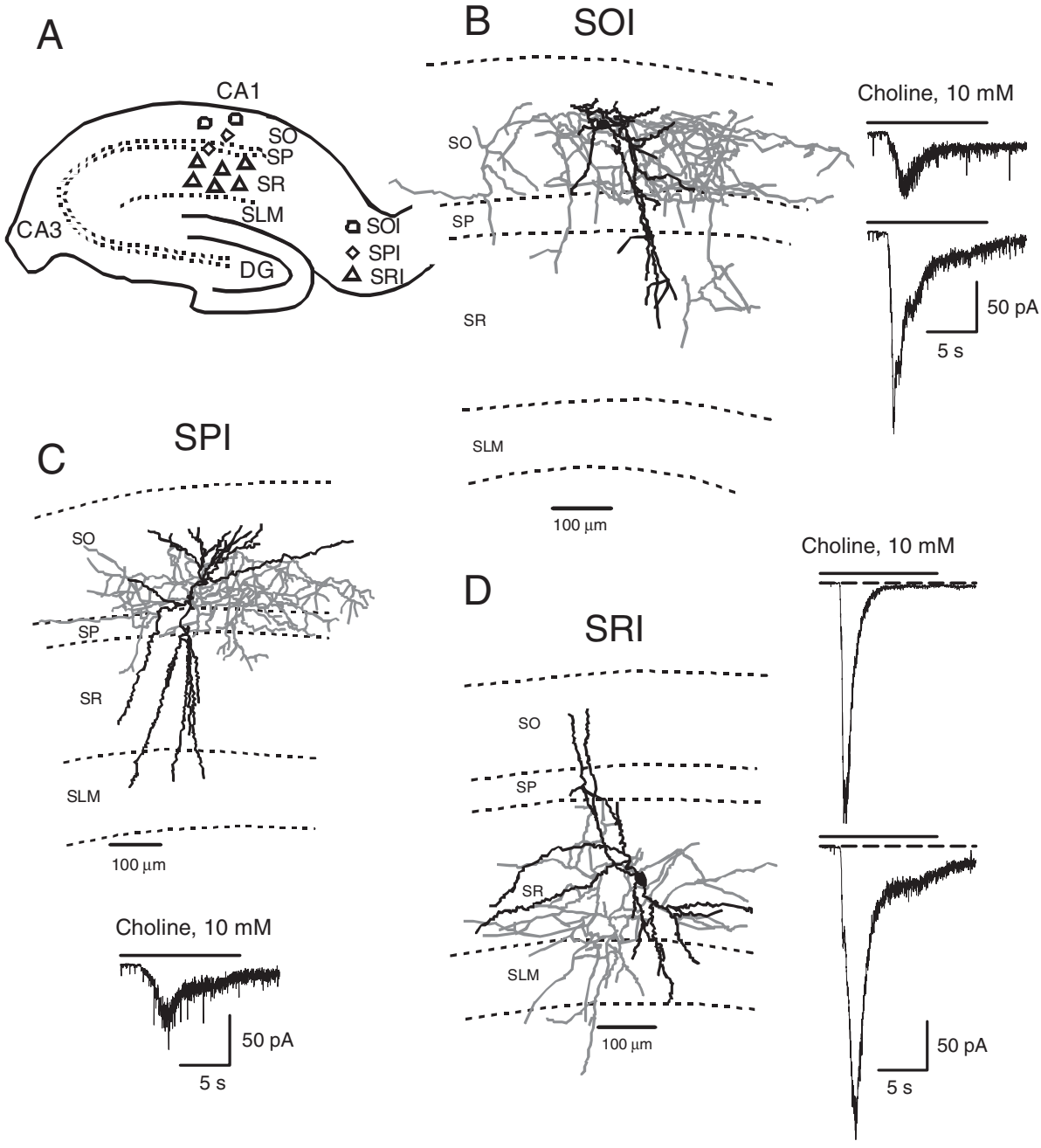

Fig. 1. Type IA currents in various interneurons in the CA1 region of guinea pig hippocampal slices. A, scheme of a hippocampal slice illustrating the approximate location of various interneuron types studied in the CA1 region. B, Neurolucida drawing of a biocytin-filled SOI showing that the axon is primarily projecting in the SO region. Sample recording of type IA current recorded from two SOIs are shown on the right. C, Neurolucida drawing of a biocytin-filled SPI showing that the axon is primarily projecting in the pyramidal cell layer. Sample recording of type IA current recorded from SPIs is shown at the bottom. D, Neurolucida drawing of a biocytin-filled SRI showing that the axon is targeted primarily to the SR region. Sample recording of type IA currents recorded from SRIs either decayed completely during agonist pulse (top trace) or had some steady-state current at the end of the agonist pulse (bottom trace). Dendrites are shown in black and axons in gray in all Neurolucida drawings.

of images of biocytin-filled neurons confirmed the identity and location of the various interneurons (Fig. 1, B–D). SOIs had their somata located in SO, dendrites branching in SR and SO, and axons projecting mainly in SO. SPIs had their somata located near the pyramidal cell body layer, multiple long dendrites traversing through the SR and the SLM, and dendrites branching in the SO. SPI axons projected mainly to the pyramidal cell body layer. SRIs had their somata located in the SR, dendrites in the SR, the SLM, and the SO, and axon projecting to the SR, the SLM, and the SO. The morphological features of SOIs, SPIs and SRIs resemble those reported for SO bistratified cells, CA1 basket cells, and SR bistratified cells, respectively (Freund and Buzsáki, 1996). In general, detailed characterization of nAChRs was carried out in SRIs.

Nicotinic Responses Recorded from Interneurons in the CA1 Field of Guinea Pig Hippocampal Slices. Interneurons in the different layers of the CA1 field of the hippocampus responded to choline with rapidly decaying nicotinic currents (Fig. 1). Choline-evoked currents either decayed completely to the baseline during the agonist pulse (see top trace in Fig. 1D) or retained some residual amplitude at the end of the agonist pulse (see bottom trace in Fig. 1D).

As described hereafter, the pharmacological properties of the choline-evoked currents recorded from CA1 interneurons in guinea pig hippocampal slices resembled those of responses referred to as type IA, which are subserved by α7 nAChRs. In the guinea pig hippocampal slices, as in rat hippocampal slices (Alkondon et al., 1999), ACh (1 mM, 12 s) and choline (10 mM, 12 s) were equally effective in evoking rapidly decaying currents (Fig. 2, A–D). When both agonists were tested in the same SRI ($n = 5$), ACh (1 mM) evoked currents that had peak amplitudes between 90 and 95% of those of currents induced by choline (10 mM). Under control conditions, there was a significant run-down of the amplitudes of choline- or ACh-induced currents; at 60 min after the beginning of the recordings, the amplitudes of choline- or ACh-evoked currents were approximately 35 to 45% of the amplitudes of the responses evoked by the first agonist pulse (data not shown).

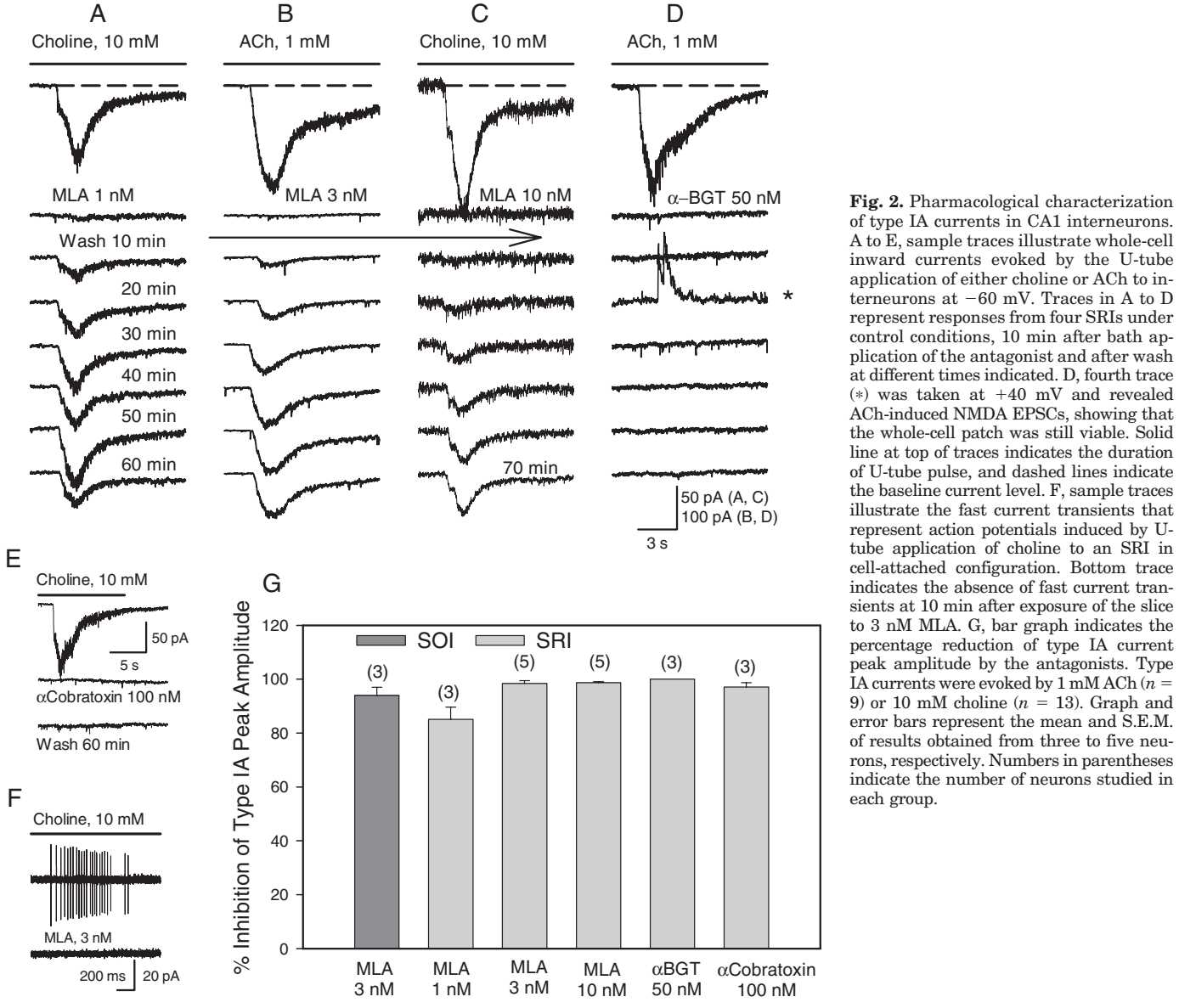

Fig. 2. Pharmacological characterization of type IA currents in CA1 interneurons. A to E, sample traces illustrate whole-cell inward currents evoked by the U-tube application of either choline or ACh to interneurons at −60 mV. Traces in A to D represent responses from four SRIs under control conditions, 10 min after bath application of the antagonist and after wash at different times indicated. D, fourth trace (*) was taken at +40 mV and revealed ACh-induced NMDA EPSCs, showing that the whole-cell patch was still viable. Solid line at top of traces indicates the duration of U-tube pulse, and dashed lines indicate the baseline current level. F, sample traces illustrate the fast current transients that represent action potentials induced by U-tube application of choline to an SRI in cell-attached configuration. Bottom trace indicates the absence of fast current transients at 10 min after exposure of the slice to 3 nM MLA. G, bar graph indicates the percentage reduction of type IA current peak amplitude by the antagonists. Type IA currents were evoked by 1 mM ACh ($n = 9$) or 10 mM choline ($n = 13$). Graph and error bars represent the mean and S.E.M. of results obtained from three to five neurons, respectively. Numbers in parentheses indicate the number of neurons studied in each group.

A 10-min exposure of the slices to 1 nM MLA decreased by 85% the amplitude of choline- or ACh-evoked currents (Fig. 2, A and G). A near complete inhibition of choline- and ACh-induced inward currents was achieved when the slices were exposed for 10 min to 3 or 10 nM MLA (Fig. 2, B, C, and G). Both peak and steady-state currents were inhibited by 1 to 10 nM MLA (Fig. 2, A–C). Choline-evoked currents recorded from SRIs and SOIs were equally sensitive to inhibition by MLA (1–10 nM). Reversal from MLA-induced inhibition depended on the antagonist concentration. After inhibition of the currents with 1 or 3 nM MLA, maximal reversal was achieved in approximately 50 min after washing the slices with MLA-free ACSF; the maximal amplitudes of the currents after the wash were approximately 35 to 45% of the currents evoked by the first agonist pulse before perfusion of the slices with MLA-containing ACSF. On average, it took 70 min or longer to reverse the inhibition induced by 10 nM MLA (see Fig. 2C).

Exposure of the slices to α-BGT (50 nM) for 10 min inhibited both choline- and ACh-induced currents in SRIs and SOIs (see Fig. 2, D and G); reversal of the inhibition was not achieved even after 1 h of washing the slices with α-BGT-free ACSF. Likewise, exposure of the slices to α-cobratoxin (100 nM) for 10 min resulted in a long-lasting inhibition of choline-evoked currents (Fig. 2E).

The ability of choline to excite SRIs was tested using the cell-attached configuration of the patch-clamp technique. U-tube application of choline to SRIs under this condition induced fast current transients that corresponded to action potentials (Fig. 2F). Bath application of 3 nM MLA blocked the excitatory effect of choline. Like in the whole-cell current measurements, the inhibitory effect of MLA was reversed after 50 min of washing the neurons with MLA-free ACSF (data not shown).

As in hippocampal slices from rats and mice (Jones and Yakel, 1997; Alkondon et al., 1999; McQuiston and Madison, 1999), the peak amplitude of choline-evoked type IA currents recorded from CA1 SRIs in guinea pig hippocampal slices increased linearly with membrane voltage in the hyperpolarizing direction (Fig. 3). The concentration dependence of choline to evoke type IA currents in CA1 SRIs of guinea pig hippocampal slices was also indistinguishable from that reported for rat hippocampal slices (Alkondon et al., 1999); the EC_{50} for choline was approximately 3.1 mM (Fig. 3). However, the amplitudes of type IA currents recorded from CA1 SRIs were on average larger in guinea pig than in rat or mouse hippocampal slices (Table 2). The mean peak amplitude of choline (10 mM)-evoked type IA currents was in the order guinea pig > rat > mouse in age-matched groups of animals (Table 2).

In 25% SRIs (12 of 48 neurons), U-tube application of ACh (0.1 or 1 mM) resulted in activation of slowly decaying inward currents at −60 mV (Fig. 4A). Application of choline (10 mM) always evoked fast-decaying, type IA currents in the neurons where ACh elicited slowly decaying currents. The slowly decaying currents remained unaffected after 10-min perfusion of the slices with ACSF containing 3 or 10 nM MLA, 50 nM α-BGT, or 100 nM α-cobratoxin (Fig. 4A). However, such currents could be reversibly inhibited by 10 μM dihydro-β-erythroidine (Fig. 4A). These currents have the pharmacological profile of α4β2 nAChR-mediated responses and are hereafter referred to as type II. In the absence of

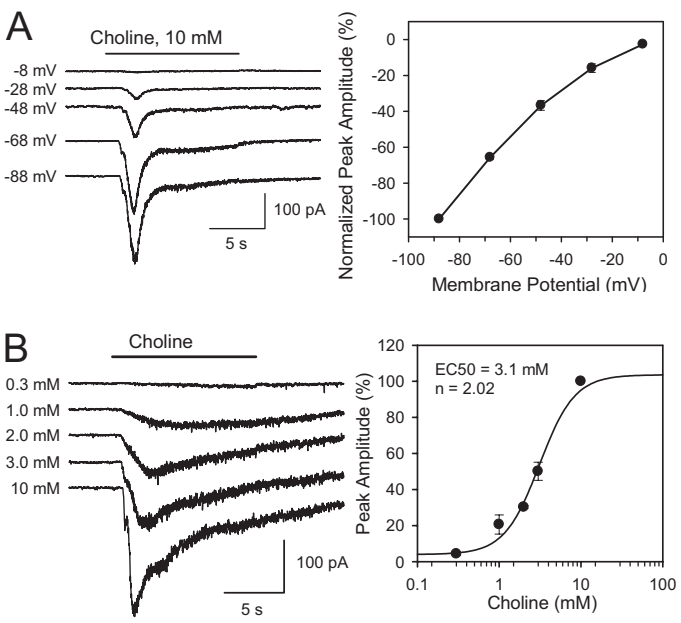

Fig. 3. Voltage dependence and agonist sensitivity of type IA currents in SRIs. A, left, sample recordings represent inward whole-cell currents induced by U-tube-applied choline at different membrane potentials. Right, plot of normalized type IA current peak amplitude versus membrane potential. Data are mean ± S.E.M. values from three neurons. In each neuron, the peak amplitude of type IA current at −88 mV was taken as 100% and used to normalize the amplitude recorded at various membrane potentials. B, left, sample recordings represent inward whole-cell currents induced by different concentrations of choline. Right, normalized peak amplitude of type IA currents is plotted against agonist concentration. The peak amplitude by 10 mM choline was taken as 100% in each neuron. Symbols and error bars represent mean and S.E.M., respectively, of results obtained from four SRIs. Solid line passing through the symbols represents the best fit of the data to a Hill equation.

pharmacological antagonists, type II currents were identified solely on the basis of the high ratio of current amplitude or net charge of inward currents evoked by 0.1 mM ACh to those evoked by 10 mM choline. The ratio of the amplitude and net charge of currents evoked by ACh to those induced by choline in 12 neurons that had presumed type II currents was 0.751 ± 0.157 and 1.425 ± 0.266, respectively, and remained significantly higher ($p < 0.001$ by Mann-Whitney test) than the ratio of the responses evoked by ACh to those induced by choline in neurons that exhibited only type IA currents.

When SRIs were voltage-clamped at +40 mV, U-tube application of ACh (0.1 mM) elicited isolated or overlapping NMDA EPSCs (21 of 22 neurons). This is confirmed by the ability of 2-amino-5-phosphonovaleric acid to abolish ACh-induced EPSCs (Fig. 4B). Bath application of either mecamylamine (3 μM, Fig. 4B) or bupropion (10 μM, data not shown) to the slices reduced the magnitude of ACh-elicited NMDA EPSCs. These responses have the pharmacological characteristics of those mediated by α3β2β4 nAChRs and herein are referred to as type III (Alkondon and Albuquerque, 2005).

Factors That Influence the Magnitude of Type IA Currents Recorded from CA1 Interneurons. The amplitudes of choline-evoked currents recorded from SOIs and SPIs were small compared with those recorded from SRIs (Fig. 1, B–D). The amplitudes of choline-evoked currents from SOIs of eight control animals ranged between 8 and 482 pA [mean ± S.E.M. = 90 ± 56 pA (n = 8 neurons) or 33.9 ± 8.8 pA, after excluding one outlier]. The current amplitudes

TABLE 2

Comparison of magnitude of CA1 SRI-type IA currents in hippocampal slices of various species of animals

For consistency, data collected using the same agonist application system (U-tube in this case) to induce type IA currents were included here. Numbers in parentheses represent the number of neurons studied.

Species	Peak Amplitude	Net Charge
	pA (mean ± S.E.M.)	*pC (mean ± S.E.M.)*
Mouse (21–22 days)[a]	9.5 ± 1.2 (26)	16 ± 1.2 (17)
Sprague-Dawley rat (17 days)[b]	98.1 ± 31.2 (15)	302 ± 102 (15)
Sprague-Dawley rat (56–68 days)[b]	165 ± 28.1 (8)	446 ± 103 (8)
August Copenhagen Irish rat* (21–22 days)[c]	47.2 ± 8.9 (33)	120 ± 18.5 (30)
Guinea pigs (16–19 days)[d]	156 ± 46.7 (18)	631 ± 151 (18)

* Both males and females were used in this study. In all other studies mentioned above, only male animals were used.
[a] Alkondon et al. (2004).
[b] Alkondon et al. (2007a).
[c] Alkondon et al. (2007b).
[d] This study.

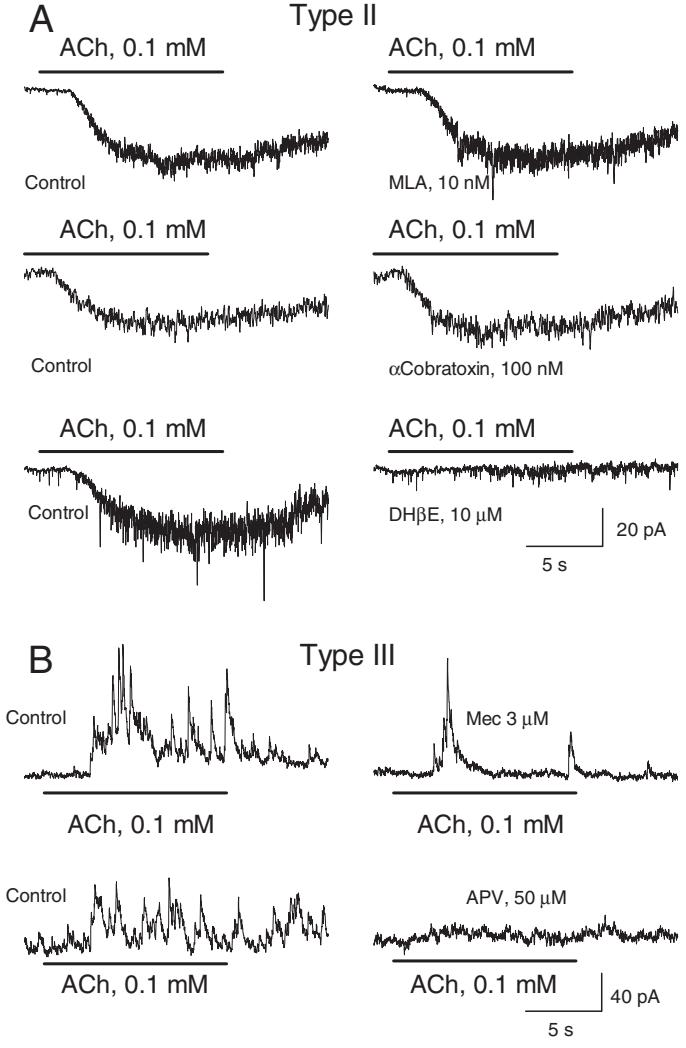

Fig. 4. Pharmacological characterization of types II and III nAChR responses in SRIs. A, sample recordings of inward whole-cell currents evoked by application of ACh to three SRIs at −60 mV before (left traces) or 10 min after bath application of the antagonists (right traces). B, sample recordings of ACh-induced NMDA EPSCs obtained from two SRIs at +40 mV before (left traces) or 10 min after bath application of the antagonists (right traces).

recorded from SPIs of three control animals were 22, 35, and 50 pA (mean ± S.E.M. = 35.6 ± 8.0 pA, n = 3 neurons). On the other hand, the current amplitudes recorded from SRIs from 25 control animals ranged widely between 11 and 874 pA (mean ± S.E.M. = 135 ± 18.8 pA, n = 60 neurons).

As mentioned above, choline-evoked currents either decayed completely to the baseline during the agonist pulse or retained some residual amplitude at the end of the agonist pulse. In SRIs, the residual current amplitude remaining at the end of the agonist pulse depended on the depth of the neurons in the slices (Fig. 5). A significant positive correlation was found between the type IA steady-state current amplitude and the depth of the SRIs and their dendrites in the slices (Fig. 5A). Although in a few slices some surface SRIs responded to choline with type IA currents that had very large peak amplitudes, data collected from several slices indicated that the depth of the SRIs did not correlate to any significant extent with the peak amplitude of type IA currents (Fig. 5B). These results suggested that the depth at which neurons are located affects the decay phase of type IA currents and, therefore, the wave form of the currents (see traces in Figs. 1 and 2), but not the peak amplitude of the currents.

The amplitudes of type IA currents recorded from SRIs with mixed type IA-type II responses, referred to as type II neurons, were smaller than those recorded from SRIs that responded to ACh or choline exclusively with type IA currents, referred to as type IA neurons (Fig. 5C). As the distance of the type IA neurons from the pyramidal cell layer increased, there was also an increase in the peak amplitudes of type IA currents. Thus, the plot of the distance of type IA neurons from the pyramidal layer versus type IA peak amplitude resulted in a positive slope that is statistically significant (Fig. 5D). A significant positive correlation was also detected between the distance of type II neurons from the pyramidal layer and the peak amplitude of type IA currents (Fig. 5E). In the age range between 11 and 26 postnatal days, type IA peak amplitudes did not show any significant age dependence (Fig. 5F).

Reports that functional α7 nAChRs can be found on dendrites of hippocampal neurons (Alkondon et al., 1996; Khiroug et al., 2003) led to the analysis of the dependence of type IA current amplitude on SRI dendrite length. SRIs that responded to choline (10 mM) with type IA peak amplitudes smaller than 50 pA or larger than 300 pA had average dendritic length of 2303 ± 264 (n = 9) and 2628 ± 321 (n = 6) μm, respectively. Thus, the peak amplitude of type IA currents did not correlate with the total dendrite length of the CA1 SRIs in the guinea pig hippocampal slices. However, examination of images of biocytin-filled SRI revealed that the thickness of initial dendrites correlates well with the size of type IA currents. As illustrated in Fig. 6, SRIs with one or

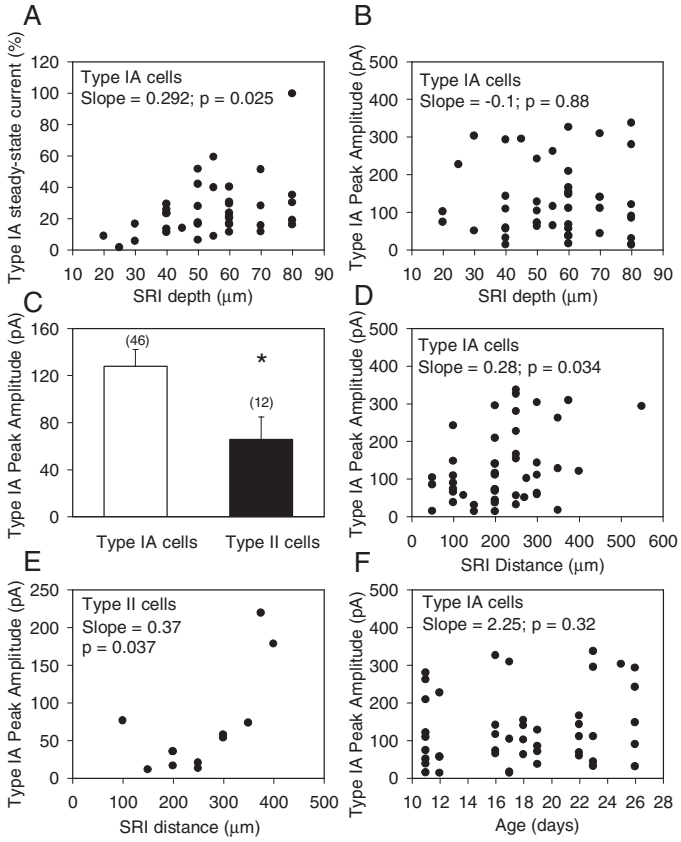

Fig. 5. Physiological factors that influence the magnitude of SRI type IA currents. A, relationship between depth of SRIs from the slice surface and the magnitude of type IA steady-state current. The amplitude of type IA current remaining at 10 s after activating the solenoid valve for agonist delivery is expressed as percentage of the peak current and is shown in the ordinate. SRI depth shown on the abscissa represents the depth of the cell body from the surface of the slice, measured just before making the recordings. Each symbol represents a single neuron. A nonparametric linear regression of the data yielded a statistically significant positive slope. Type IA cells mentioned in all places represent those SRIs exhibiting only type IA currents. B, relationship between depth of SRIs from the slice surface and type IA current peak amplitude. A nonparametric linear regression of the data indicated no significant correlation between the two parameters. C, bar graph shows the peak amplitude of type IA currents in type IA neurons (neurons that exhibit only type IA currents) and in type II neurons (neurons with mixed responses). Numbers in parentheses represent the number of neurons studied. Graph and error bar are mean and S.E.M., respectively, of results obtained from 46 type IA cells and 12 type II cells. $*$, results are different with $p = 0.038$ (Student's t test). D and E, relationship between SRI distance from the pyramidal layer and type IA current peak amplitude in type IA (D) and type II (E) cells. The distance was measured from the midline of the pyramidal cell layer to the center of the SRI before making the recordings in the slices. In both cases, a nonparametric linear regression of the data revealed a statistically significant positive slope. F, relationship between the age of guinea pigs and type IA current peak amplitude.

more thick initial dendrites (diameter between 3 and 5 μm) responded to 10 mM choline with large-amplitude type IA currents, whereas those with thin initial dendrites (diameter between 1 and 2 μm) responded to 10 mM choline with small amplitude type IA currents. Statistical comparison of the peak amplitude of type IA currents recorded from SRIs with thick versus thin dendrites revealed a highly significant ($p < 0.002$ by Mann-Whitney test) difference (Fig. 6, bottom).

Effects of Acute Treatment of Guinea Pigs with Soman and/or Galantamine on Type IA Currents in CA1 SRIs. To assess the degree of AChE inhibition in the hippocampal slices at the functional level, the ratio of peak amplitude or net charge of type IA currents induced in each SRI by ACh at 0.1 mM (nearly one-tenth of saturating concentration of 1 mM) and choline at 10 mM (nearly saturating concentration) was calculated. If ACh hydrolysis by AChE is a rate-limiting step in the termination of responses evoked by exogenous application of ACh to the slices, AChE inhibition would result in enhancement of ACh- but not choline-induced currents. Consequently, the magnitude of the ratio of ACh- to choline-evoked type IA currents would increase. Using this rationale, the ratio of the peak amplitude or net charge of ACh- to choline-induced type IA currents (herein referred to as ACh/choline peak amplitude or net charge ratio) recorded from CA1 SRIs in slices of control animals was compared with that recorded from corresponding interneurons in slices obtained from guinea pigs at various times after their treatments. In nearly half of the experiments, type IA currents were confirmed by the application of 3 to 10 nM MLA to the slices at the end of the protocol.

Approximately 75% of the guinea pigs that received a subcutaneous injection of 1× LD_{50} soman presented clear signs of acute OP intoxication. Facial twitches, chewing, slight hyperlocomotion, head tremors, profuse secretions, muscle fasciculations, rearing, strong grinding, gnashing or clenching of the teeth (bruxism), all limb clonus, and convulsions were common signs observed in the majority of the animals challenged with 1× LD_{50} soman. Between 10 min and 2 h after the challenge with 1× LD_{50} soman, the toxic signs progressed from the peripheral nicotinic and muscarinic effects to the central nervous system effects. Convulsions triggered by 1× LD_{50} soman became life-threatening when they occurred unremittingly and lasted longer than 10 min or when they recurred for longer than 10 min without the animals regaining consciousness during the interictus interval. There is evidence that 10 min of continuous convulsions is sufficient to damage neurons and that unremittingly or recurrent seizures lasting longer than 10 min are unlikely to self-terminate (DeLorenzo et al., 1999; García Peñas et al., 2007). Thus, following the Institutional Animal Care and Use Committee guidelines, the animals were euthanized as soon as the life-threatening generalized unremittingly or recurrent convulsions developed.

At 24 h after the soman challenge, the surviving guinea pigs had lost 10 to 15% of their initial weight and could be divided into four general groups. One group consisted of animals that still presented sporadic convulsions even without handling. The second group consisted of animals that developed convulsions only during handling. The third group consisted of animals that showed hyperlocomotion in their cages but had no convulsions at rest or during handling. The fourth group consisted of animals whose gross behavior was comparable with that of control animals. At 7 and 14 days after the soman challenge, the guinea pigs were gaining weight at a lower rate than control animals (data not shown), although they could not be distinguished on the basis of their gross behavior from control animals.

As reported before (Albuquerque et al., 2006), guinea pigs that received an i.m. injection of galantamine (8 mg/kg) presented no immediate weight loss, gained weight at the same rate as control animals, and showed no alteration of gross behavior. In addition, as reported earlier (Pereira et al., 2008), guinea pigs that were treated with galantamine (8 mg/kg i.m.) and subsequently challenged with 1× LD_{50} soman showed approximately 10% of weight loss at the first

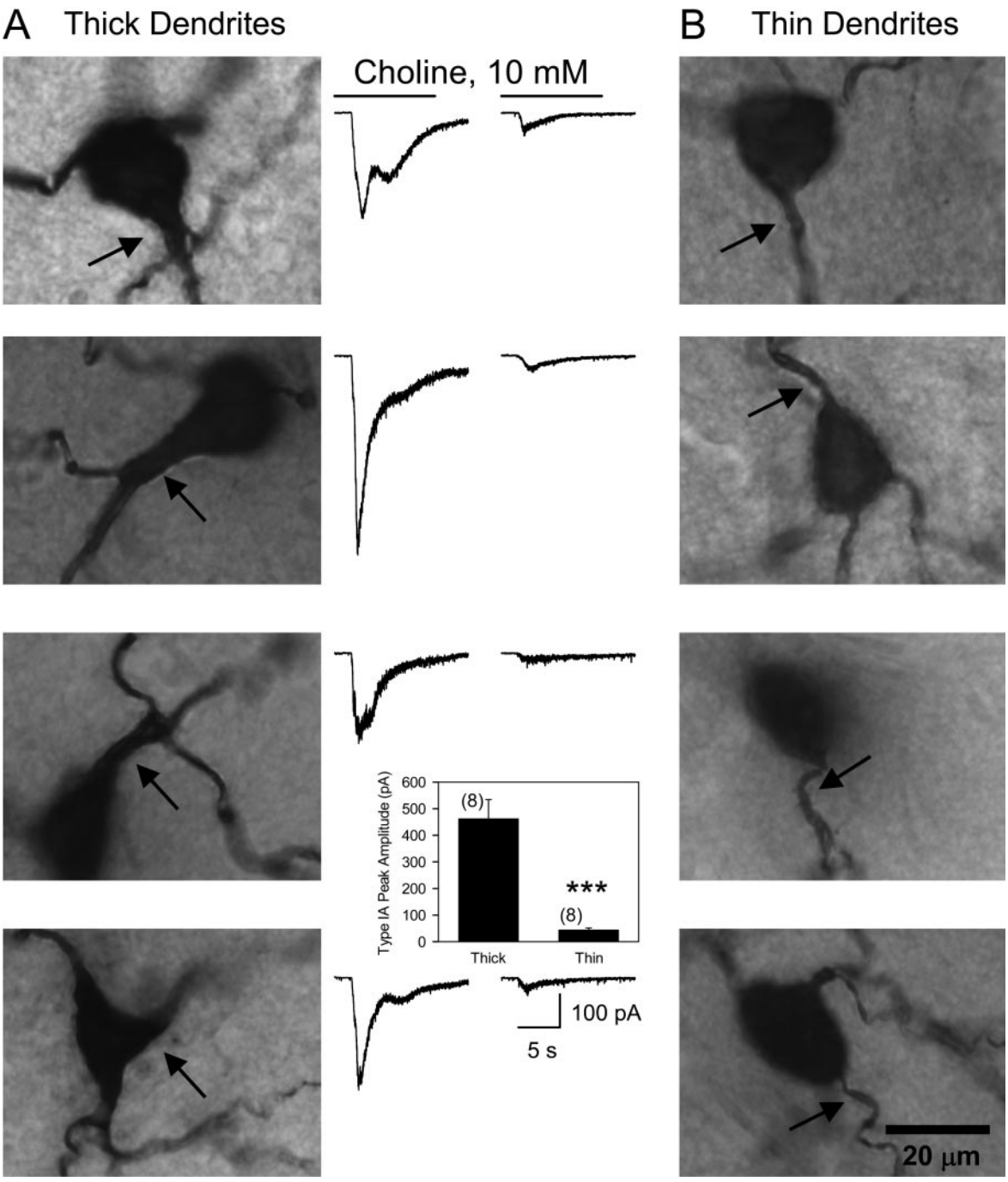

Fig. 6. Relationship between dendrite initial segment thickness and type IA current peak amplitude in SRI. A, photographs of biocytin-filled SRIs reveal thick segments of initial dendrites (indicated by arrows) emerging from the cell body. Traces shown to the right of each photograph represent type IA currents recorded from that particular neuron. B, photographs of biocytin-filled SRIs reveal thin segments of initial dendrites (indicated by arrows) emerging from the cell body. Calibration line in the last photomicrograph applies to all images. Traces shown to the left represent type IA currents recorded in each neuron. Calibration at the bottom applies to all traces. Inset, graph of the peak amplitudes of type IA currents recorded from SRIs with thin (1–2 μm thick) or thick (3–5 μm thick) initial dendritic segments. ***, $p < 0.002$ by Mann-Whitney test.

24 h after the challenge. However, by 7 and 14 days after the challenge, they were gaining weight at the same rate as control animals and showed no alteration of gross behavior (data not shown).

In hippocampal slices obtained from control animals, the ACh/choline peak amplitude and net charge ratio recorded from CA1 SRIs were 0.067 ± 0.009 and 0.135 ± 0.021, respectively ($n = 31$ neurons). In hippocampal slices obtained from animals at 1 day after a single injection of soman, the ratios were significantly larger than those recorded from SRIs in slices from age-matched control animals (Fig. 7). On the other hand, the ACh/choline peak amplitude and net charge ratios recorded from SRIs in slices obtained from guinea pigs at 7 and 14 days after the soman challenge were comparable with those recorded from SRIs of age-matched control animals, suggesting that AChE activity had returned to control levels.

The ACh/choline peak amplitude and net charge ratios recorded from SRIs in slices obtained at 1, 7, or 14 days after

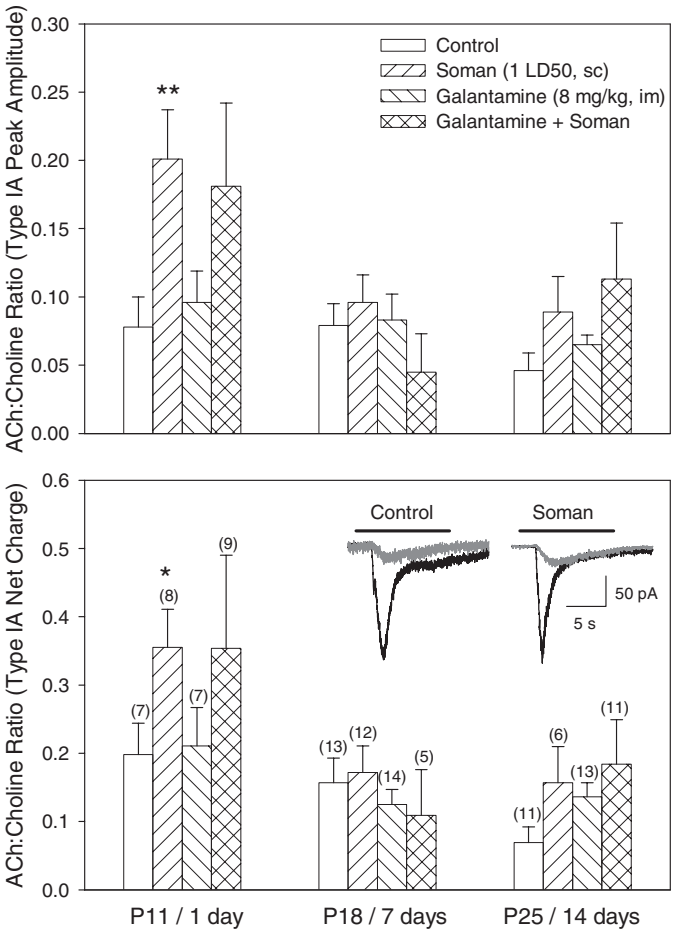

Fig. 7. Effects of the acute treatment with galantamine and/or soman on the magnitude of the ratio of ACh- to choline-evoked type IA currents in SRIs. The ratios of ACh (0.1 mM)- to choline (10 mM)-evoked type IA peak amplitudes (top) or net charge (bottom) from several SRIs are shown for the different ages of untreated guinea pigs and for the various times after their treatments with galantamine (8 mg/kg i.m.) and/or soman (1× LD_{50} s.c.). It was assumed that AChE inhibition in the slices would modify only the response evoked by the subsaturating concentration of ACh and, therefore, change the ACh/choline ratio. Graph and error bars are mean and S.E.M., respectively, of results obtained from different neurons. Numbers in parentheses represent the number of SRIs in each group. Inset trace pairs shown in the bottom graph are representative samples of type IA currents induced by 10 mM choline (black traces) or 0.1 mM ACh (gray traces) in a given SRI in the control and soman group. The animals were treated as described under *Material and Methods*. *, $p = 0.05$; **, $p = 0.006$ compared with control by Mann-Whitney test.

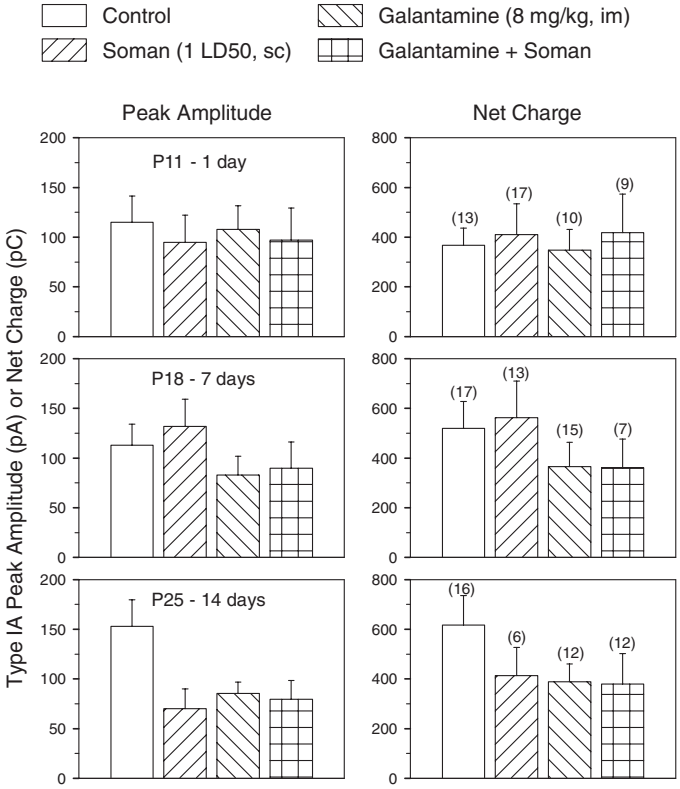

Fig. 8. Effect of the acute treatments with galantamine and/or soman on choline-evoked type IA currents in CA1 SRIs. Graph of peak amplitudes (left graphs) or net charge (right graphs) of type IA currents recorded from SRIs in hippocampal slices taken from animals at different ages or at various times after a given treatment. The net charge of type IA currents was calculated for 12 s of the trace starting from the trigger applied at the solenoid valve. Only type IA cells were included in this analysis. Control group of animals were in the age ranges of P11 to P12 (top), P16 to P19 (middle), and P25 and P26 (bottom). Drug-treated groups were age-matched to controls and obtained 1, 7, or 14 days (top, middle, and bottom, respectively) after any given treatment. Graph and error bars are mean and S.E.M., respectively, of results from seven to 17 neurons. Numbers in parentheses represent the number of neurons studied in each experimental group.

the acute treatment of the guinea pigs with galantamine were comparable with those recorded from SRIs of age-matched control animals (Fig. 7). In guinea pigs that received galantamine before soman, the ACh/choline ratio in type IA current amplitude and net charge remained elevated above control values. However, the difference from control was not statistically significant (Fig. 7).

At 1, 7, or 14 days after the acute challenge of the guinea pigs with 1× LD_{50} soman, the amplitudes and net charge of choline-evoked currents recorded from SRIs were comparable with those recorded from SRIs in slices of age-matched control animals (Fig. 8). Likewise, acute treatment with galantamine or pretreatment with galantamine followed by the challenge with soman failed to alter the magnitude of choline-evoked type IA current (Fig. 8). In contrast, after the soman challenge, the amplitude and net charge of choline-evoked type IA currents recorded from CA1 SOIs were smaller than those recorded from neurons of control animals (see Fig. 9).

Effects of Acute Treatment of Guinea Pigs with Soman and/or Galantamine on Type II Currents in CA1 SRI. Examination of the animals in each treatment group, without considering the age and time after treatment, revealed that the percentage of SRIs that responded to 0.1 mM ACh with type II currents was similar in control and soman-challenged animals (Fig. 10A). In contrast, after the treatment with galantamine, the percentage of SRIs that responded to 0.1 mM ACh with type II currents was lower than that found in control animals (Fig. 10A). In slices obtained from guinea pigs that were treated with galantamine and subsequently challenged with soman, the percentage of SRIs showing type II currents in response to 0.1 mM ACh was not statistically different from that seen in control animals (Fig. 10A).

Categorizing the results according to the age of control animals or time after the soman challenge revealed that at 1 day after the exposure to soman, there was an increase in the percentage of SRIs that responded to ACh with type II currents (Fig. 10B). At 7 days after the challenge, the percentage

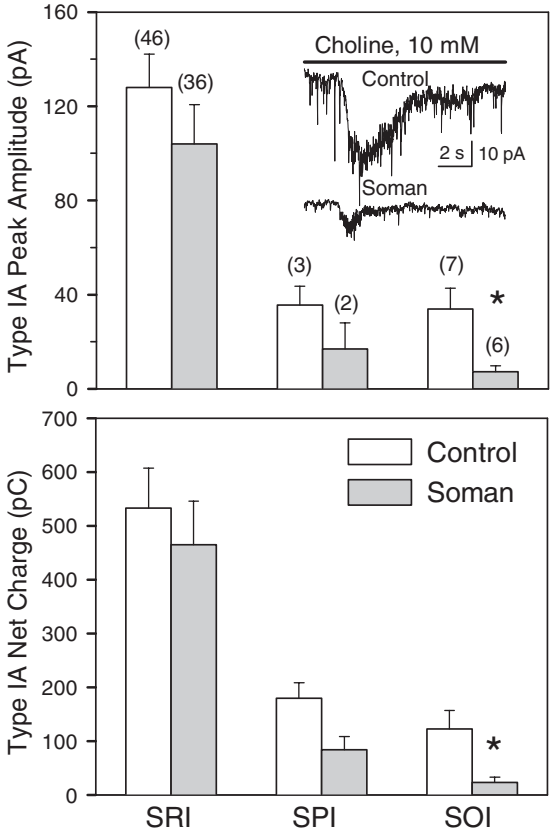

Fig. 9. Effect of the acute treatment with soman on type IA currents in different CA1 interneurons. Graph of peak amplitudes or net charge of type IA currents recorded from CA1 SRIs, SPIs, and SOIs in hippocampal slices taken from untreated or soman ($1\times$ LD_{50})-challenged guinea pigs. Data from animals at ages between P11 and P26 were pooled together for each neuron type. Inset, representative sample recordings of choline-evoked currents recorded from SOIs in hippocampal slices of untreated and soman-treated guinea pigs. Graph and error bars are mean and S.E.M., respectively, of results from various neurons. Numbers in parentheses represent the number of neurons studied in each experimental group. *, $p = 0.02$ compared with control according to the unpaired Student's t test.

of SRIs that responded to ACh with type II currents was lower than that seen in the hippocampus of age-matched control animals (Fig. 10B). At 14 days after the challenge, the percentage of SRIs exhibiting type II currents in response to ACh was comparable with that seen in age-matched control animals. Exposure to soman had no effect on the peak amplitude and net charge of type II currents evoked by 0.1 mM ACh in SRIs (see Fig. 10C).

At 1, 7, and 14 days after the acute treatment of the guinea pigs with galantamine, the percentage of SRIs exhibiting type II currents in response to ACh was significantly lower than that observed in the hippocampus of age-matched control guinea pigs (Fig. 10B). After the treatment with galantamine, soman was unable to induce alterations in the percentage of type II nAChR-positive neurons (Fig. 10B).

Effects of Acute Treatment of Guinea Pigs with Soman and/or Galantamine on Type III Currents in CA1 SRI. Type III currents were quantitatively assessed by the analysis of the net charge of ACh-evoked NMDA EPSCs in SRIs. Exposure to soman caused a significant reduction in the net charge of ACh-induced NMDA EPSCs compared with untreated guinea pigs (Fig. 11). The effect was long-lasting because it could be detected in slices obtained from guinea

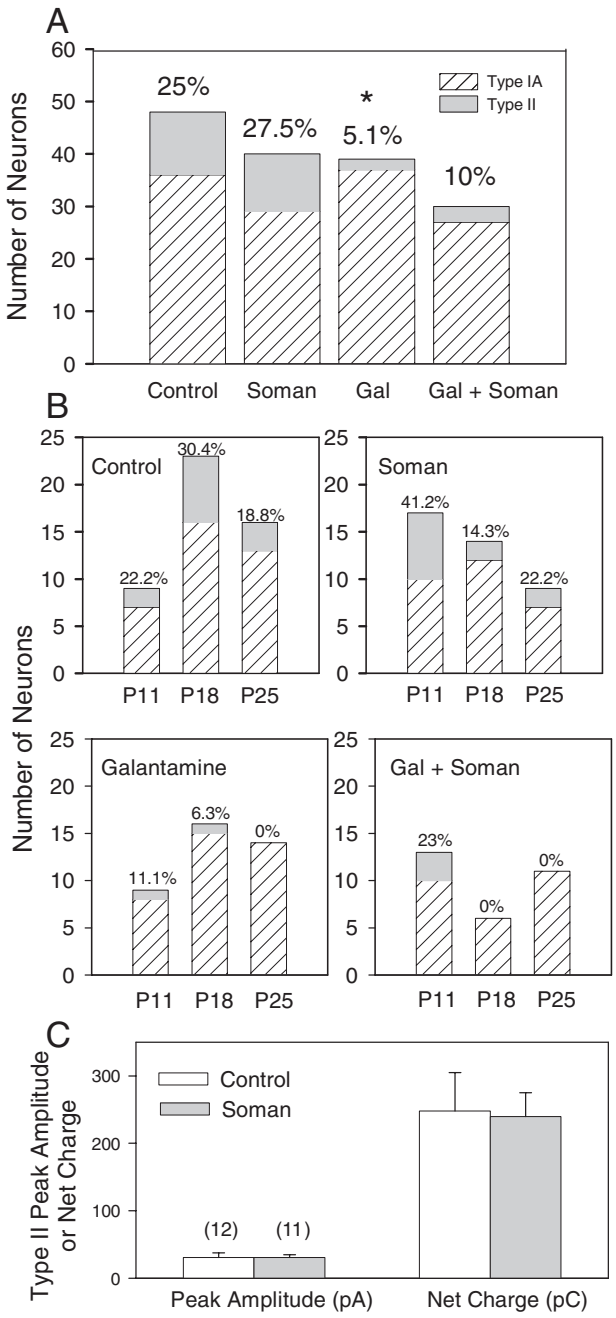

Fig. 10. Effect of the acute treatments with galantamine and/or soman on the percentage of CA1 SRIs exhibiting type II currents in response to ACh. A, bar graph depicts the percentage of CA1 SRIs that respond to ACh (0.1 mM) with type IA or type II currents in various groups of animals. Ordinate, number of neurons showing type IA or type II currents. Note that all type II current neurons also had type IA currents. The percentage of neurons responding to ACh with type II currents in each group is shown at the top. Results obtained from P11 to P26 animals were grouped together. In each treatment group, results obtained from slices taken from the guinea pigs at 1, 7, and 14 days after that treatment were pooled together. The prevalence of type II currents in CA1 SRIs of galantamine-treated animals is significantly lower compared with control by Fisher's exact test (*, $p = 0.017$). B, results for each treatment group are categorized according to the age of the animals and the time after a given treatment. C, bar graph depicts the peak amplitude and net charge of type II currents recorded from SRIs of control and soman-challenged animals. Results from all age groups were pooled together. Graph and error bars are mean and S.E.M., respectively, of results obtained from various neurons. Numbers in parentheses represent the number of neurons studied in each experimental group.

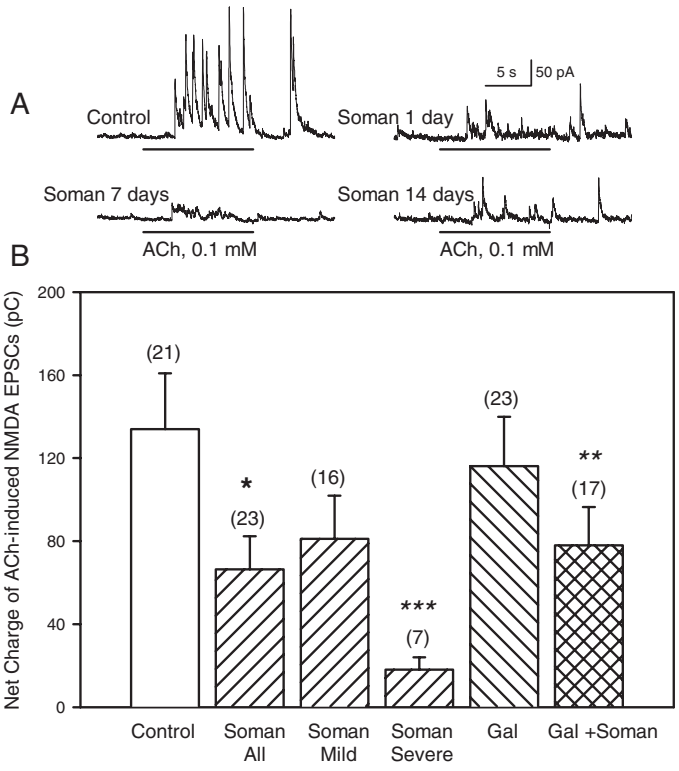

Fig. 11. Effects of acute treatments with soman and/or galantamine on type III responses recorded from CA1 SRIs. A, ACh-induced NMDA EPSCs recorded from CA1 SRI at +40 mV in hippocampal slices from different groups of animals. B, bar graph shows the magnitude of type III responses recorded from CA1 SRIs of animals subjected to various treatments. Results obtained from P11 to P26 control animals were grouped together. Drug-treated group consists of animals at 1, 7, and 14 days after a given treatment. Graph and error bars are mean and S.E.M., respectively, of results obtained from various neurons. Numbers in parentheses are the number of neurons studied in each experimental group. The groups "soman mild" and "soman severe" refer to groups of animals that presented mild reactions and severe reactions, including long-lasting intermittent convulsions. *, $p < 0.01$ and ***, $p < 0.001$ compared with control; ** $p < 0.01$ compared with soman severe by Mann-Whitney nonparametric analysis.

pigs at 1, 7, or 14 days after their challenge with 1× LD_{50} soman (Fig. 11A). In addition, the effect was clearly evident in guinea pigs that developed long-lasting convulsions in response to soman. Acute treatment of the guinea pigs with galantamine alone did not alter the magnitude of type III nAChR response to any significant extent; however, galantamine pretreatment prevented the inhibitory effect of soman on type III nAChR responses (Fig. 11B).

CA1 Interneuron Morphology in Hippocampal Slices from Guinea Pigs Acutely Challenged with Soman. Qualitative evaluation of the images of biocytin-filled neurons in the slices revealed that the axonal arborization of CA1 interneurons in the hippocampi of animals challenged with a single dose of soman was different from that seen in slices of control animals. Changes in the axonal arborization of CA1 interneurons were more pronounced in animals that presented severe convulsions after the soman challenge. The SOIs were the most affected neurons. Although in hippocampal slices of control guinea pigs, SOI axons were densely confined to the SO itself (Fig. 12A), in slices obtained at 24 h after the soman challenge, SOI axons were projecting throughout all the hippocampal layers (Fig. 12B).

Discussion

The present study demonstrates that, in the guinea pig, hippocampus α7 and α4β2 nAChRs are expressed by CA1 SRIs, SOIs, and SPIs, and α3β2β4 nAChRs control glutamatergic inputs to CA1 SRIs. An acute exposure to soman: 1) transiently enhanced ACh-induced α7 nAChR activation in CA1 SRIs, 2) reduced the α7 nAChR activity in SOIs, 3) increased the proportion of SRIs expressing α4β2 nAChRs, and 4) suppressed α3β2β4 nAChR-triggered EPSCs onto CA1 SRIs. The acute in vivo treatment with galantamine prevented soman-induced enhancement on ACh-evoked α7 nAChR currents, caused a prolonged reduction of the α4β2 nAChR activity in CA1 SRIs, and counteracted the effects of soman on α3β2β4 nAChRs. The potential contribution of these effects to the toxicity of soman and the antidotal effectiveness of galantamine are discussed herein.

nAChR Subtypes in the Guinea Pig Hippocampus. Pharmacologically distinct nAChR responses could be recorded from CA1 interneurons in the hippocampus of 11- to 26-day-old guinea pigs. As in the rat and mouse hippocampus (Jones and Yakel, 1997; Alkondon et al., 1999; McQuiston and Madison, 1999), CA1 SRIs, SOIs, and SPIs in the guinea pig hippocampus express functional α7 nAChRs. The pharmacological properties of α7 nAChR responses in the guinea pig hippocampus were comparable with those recorded from the hippocampi of other rodents. However, the amplitudes of these responses were higher in CA1 SRIs of guinea pigs than of age-matched rats and mice. It is tempting to speculate that the higher expression of functional α7 nAChRs in the hippocampus of guinea pig compared with rats and mice is indicative of the higher degree of cholinergic development in the guinea pig hippocampus.

As in the rat hippocampus (Alkondon and Albuquerque, 2005), approximately 25 to 35% of the CA1 SRIs in the guinea pig hippocampus expressed functional α4β2 nAChRs in addition to functional α7 nAChRs. Further, as in rat hippocampal slices (Alkondon and Albuquerque, 2005), all CA1 SRIs in the guinea pig hippocampus received inputs from glutamatergic neurons/axons expressing α3β2β4 nAChRs.

Intrinsic Factors That Influence α7 nAChR Activity in Guinea Pig Hippocampal Slices. At least three physiological factors appear to regulate the α7 nAChR activity/expression in guinea pig CA1 SRIs. First, the magnitude of α7 nAChR responses was smaller in neurons that also express functional α4β2 nAChRs than in those expressing exclusively functional α7 nAChRs.

Second, the magnitude of α7 nAChR responses recorded from guinea pig CA1 SRIs increased with the distance of the neurons from the pyramidal layer and was greater than that recorded from SOIs or SPIs. In the rat hippocampus, α7 nAChR regulation of GABAergic transmission was also found to be higher in the CA1 SLM field of the hippocampus (Alkondon and Albuquerque, 2001). Therefore, the degree of α7 nAChR expression in the hippocampal interneurons is layer dependent.

Third, the α7 nAChR activity in guinea pig CA1 SRIs increased with the thickness of the initial segments of the neuronal dendrites. In these neuronal compartments, α7 nAChRs could serve as targets for cholinergic synaptic connections. Only few ACh varicosities have been found to make

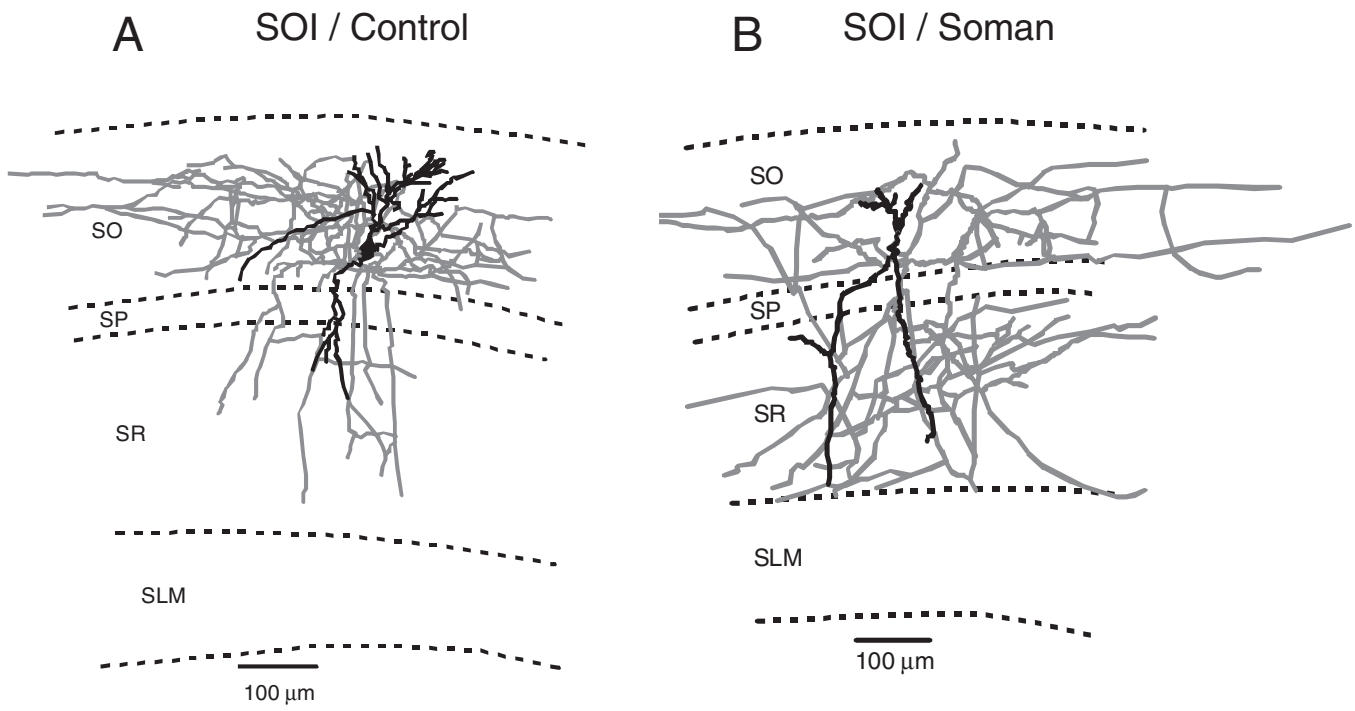

Fig. 12. Changes in CA1 SOI morphology after injections of soman. Neurolucida drawings of biocytin-filled CA1 SOIs of a control and a soman (1× LD_{50})-challenged guinea pig 1 day after an acute treatment with soman. SOI axons are largely confined to the SO in control animals and largely sprouted to the SO, stratum pyramidale, and SR in soman-challenged animals.

synaptic contacts within the rat hippocampus, and most of these synaptic contacts occur predominantly on the dendritic branches, not spines (Aznavour et al., 2005).

Influence of AChE on nAChR Activity in Guinea Pig Hippocampal Slices. It has been reported that AChE activity in the hippocampus is reduced to approximately 25% of control levels at 1 h after an acute exposure of guinea pigs to 1× LD_{50} soman, shows very little sign of recovery at 24 h after the exposure, and slowly recovers to approximately 60% of control levels at 7 days after the challenge (Lintern et al., 1998). In contrast, after an acute treatment of guinea pigs with galantamine (8 mg/kg i.m.), brain AChE activity is reduced to no more than 25% in the 1st hour and returns to control levels within 6 h (Albuquerque et al., 2006).

At 24 h after the acute in vivo challenge of the guinea pigs with 1× LD_{50} soman, the ACh/choline amplitude and net charge ratios were increased, whereas the magnitude of choline-evoked type IA currents was unaltered. At the same time, the magnitude of α7 nAChR responses was decreased in SOIs. These results suggest that AChE is a rate-limiting factor for the termination of α7 nAChR activation by exogenously applied ACh in guinea pig hippocampal slices. The differential level of AChE activity and cholinergic innervation in both layers can result in the layer-specific effects of enzyme inhibition on α7 nAChR activation by exogenous agonists.

The degree of cholinergic innervation and the AChE activity are low in the SR and high in the SO (Geneser-Jensen, 1972; Schäffer et al., 1998). Thus, substantial AChE inhibition, as seen at 24 h after the soman challenge (Lintern et al., 1998), can prolong the lifetime of exogenously applied ACh available to activate the α7 nAChRs in the SR. In contrast, AChE inhibition in the SO can increase the levels of endogenous ACh sufficiently to desensitize the α7 nAChRs. As a consequence, α7 nAChR responses triggered by exogenous application of ACh to SOIs will be decreased upon AChE inhibition. The prevention by galantamine of the soman-induced irreversible AChE inhibition can counteract the α7 nAChR changes induced by the nerve agent (Fig. 13).

At 1 and 7 days after the acute exposure to soman, there was an increase and a decrease, respectively, in the percentage of α4β2 nAChR-expressing SRIs in the guinea pig hippocampus. The activity of α4β2 nAChRs returned to control levels at 14 days after the soman challenge. Changes in α4β2 nAChR activity in the hippocampus of soman-exposed animals were unlikely to be related to increased levels of ACh in response to AChE inhibition, because the ACh concentration used to activate the α4β2 nAChRs was supramaximal. In addition, as indicated above (Lintern et al., 1998), a significant portion of the AChE activity is recovered in the guinea pig hippocampus at 7 days after an exposure to soman. Therefore, if levels of exogenously applied ACh were sustained longer in the slices because of AChE inhibition and consequently desensitized α4β2 nAChRs, receptor activity should have been lower at 1 than at 7 days after the soman challenge. The transient alterations in α4β2 nAChR activity in the SRIs of soman-challenged guinea pigs may be accounted for by intracellular mechanisms triggered by soman-induced direct or indirect changes in the activity of other cholinergic receptors, including α7 nAChRs (see results above) and muscarinic receptors (Silveira et al., 1990).

Involvement of nAChRs in the Actions of Soman and Galantamine. At 24 h after the soman challenge, the enhanced activities of SRI α7 and α4β2 nAChRs and the reduced SOI α7 nAChR activity can suppress nAChR-mediated feedback inhibition while allowing nAChR-mediated feedforward inhibition in the CA1 region of the hippocampus (Fig. 13). Disruption of the axonal arborization of SOIs,

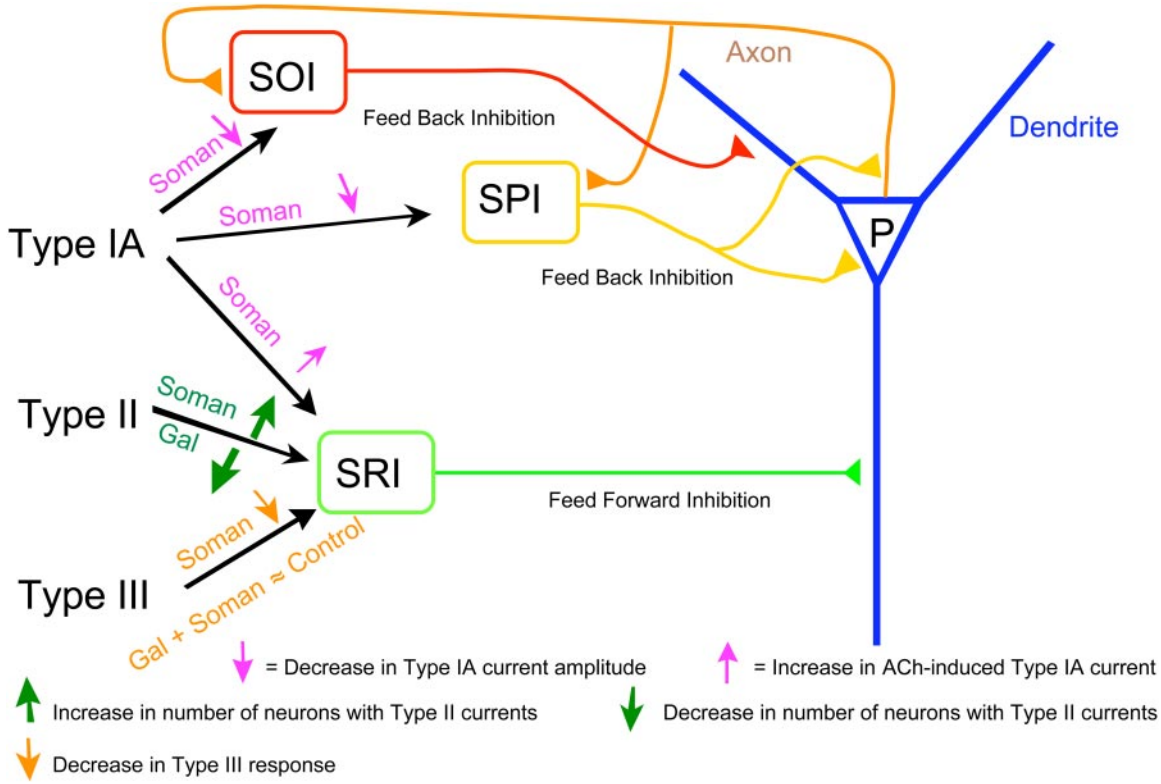

Fig. 13. Scheme illustrating the network effect of soman and galantamine. The pyramidal neuron (P) in the CA1 hippocampal region receives inhibitory inputs from various interneurons. The SRI provides the feed-forward inhibition, whereas both SOI and SPI provide feedback inhibition to the pyramidal neurons. Soman suppresses feedback inhibition (i.e., causes disinhibition) via inhibition of type IA currents in SOI and SPI. Soman enhances feed-forward inhibition via enhancement of ACh-induced type IA currents and via increase in the number of SRI with type II currents. Soman-induced imbalance in feed-forward and feedback inhibition results in increased pyramidal neuron firing leading to excitotoxicity, neuronal damage, and altered rhythm. The loss of pyramidal neurons partly contributes to a decrease in type III nAChR activity after exposure to soman. Galantamine opposes the action of soman by preventing irreversible inhibition of AChE, leading to preservation of nAChR activity, and/or by inducing changes in the expression of nAChRs in the interneurons, thereby restoring the balance of nAChR-dependent feed-forward and feedback inhibition in the hippocampal neurocircuitry.

which can also contribute to a reduction of the feedback inhibition of CA1 pyramidal neurons, was one of the most striking morphological alterations observed in the hippocampus of soman-challenged guinea pigs. Decreased feedback inhibition in the CA1 field of the hippocampus appears to facilitate synchronization of the hippocampal neuronal network and sustain epileptiform activity (Stief et al., 2007).

In galantamine-treated, soman-challenged guinea pigs, the percentage of $\alpha4\beta2$ nAChR-expressing SRIs did not change in the first 24 h after the challenge and decreased subsequently. Galantamine alone caused a long-lasting reduction of the percentage of SRIs that exhibited type II currents in response to ACh. Thus, it is tempting to speculate that the net effect seen on $\alpha4\beta2$ nAChR activity in the galantamine-treated, soman-challenged animals is the result of a functional antagonism between galantamine and soman. In addition, $\alpha7$ nAChR responsiveness of SRIs to ACh was not significantly different between guinea pigs that were pretreated with galantamine, soman-challenged, and control animals. This effect could have resulted from the protection by galantamine of the irreversible AChE inhibition by soman.

A sustained reduction of the ACh-induced NMDA EPSCs was observed in SRIs of guinea pigs that developed convulsions in response to the soman challenge. The inhibitory effect of soman on these responses does not appear to be related to changes in the concentrations of ACh that are available to activate the receptors. First, the AChE activity, but not the suppression of the $\alpha3\beta2\beta4$ nAChR-mediated responses, recovers to a substantial extent at 7 days after an acute challenge with soman (Lintern et al., 1998). Second, the effect of soman was only evident in animals that presented intermittent convulsions for long periods of time. The effect of soman on type III responses could be partly attributed to the extensive loss of CA1 pyramidal neurons that occurs after an acute exposure to the nerve agent (Albuquerque et al., 2006) because they contribute glutamate inputs to the CA1 SRIs in the slices. In fact, pretreatment with galantamine, which reportedly counteracts the soman-induced neurodegeneration (Albuquerque et al., 2006), prevented the effect of soman on ACh-induced NMDA EPSCs.

In conclusion, the results presented herein demonstrate that pretreatment of guinea pigs with galantamine counteracts the neuron type-specific effects of soman on the activity of different nAChRs known to be involved in feedback and feed-forward mechanisms that regulate the rhythms of the neuronal networks in the hippocampus.

Acknowledgments

We thank Major J. L. Goodin (United States Army Medical Research Institute of Chemical Defense) for insightful comments on the manuscript, Mabel Zelle for technical assistance, and Bhagavathy Alkondon for preparing hippocampal slices, biocytin processing, and Neurolucida drawing of biocytin-filled neurons.

References

Albuquerque EX, Deshpande SS, Kawabuchi M, Aracava Y, Idriss M, Rickett DL, and Boyne AF (1985) Multiple actions of anticholinesterase agents on chemosensitive synapses: molecular basis for prophylaxis and treatment of organophosphate poisoning. *Fundam Appl Toxicol* **5:**S182–S203.

Albuquerque EX, Pereira EFR, Aracava Y, Fawcett WP, Oliveira M, Randall WR, Hamilton TA, Kan RK, Romano JA Jr, and Adler M (2006) Effective countermeasure against poisoning by organophosphorus insecticides and nerve agents. *Proc Natl Acad Sci U S A* **103:**13220–13225.

Alkondon M and Albuquerque EX (2001) Nicotinic acetylcholine receptor α7 and α4β2 subtypes differentially control GABAergic input to CA1 neurons in rat hippocampus. *J Neurophysiol* **86:**3043–3055.

Alkondon M and Albuquerque EX (2004) The nicotinic acetylcholine receptor subtypes and their function in the hippocampus and cerebral cortex. *Prog Brain Res* **145:**109–120.

Alkondon M and Albuquerque EX (2005) Nicotinic receptor subtypes in rat hippocampal slices are differentially sensitive to desensitization and early in vivo functional up-regulation by nicotine and to block by bupropion. *J Pharmacol Exp Ther* **313:**740–750.

Alkondon M, Pereira EFR, and Albuquerque EX (1996) Mapping the location of functional nicotinic and γ-aminobutyric $acid_A$ receptors on hippocampal neurons. *J Pharmacol Exp Ther* **279:**1491–1506.

Alkondon M, Pereira EFR, Barbosa CT, and Albuquerque EX (1997) Neuronal nicotinic acetylcholine receptor activation modulates γ-aminobutyric acid release from CA1 neurons of rat hippocampal slices. *J Pharmacol Exp Ther* **283:**1396–1411.

Alkondon M, Pereira EFR, Eisenberg HM, and Albuquerque EX (1999) Choline and selective antagonists identify two subtypes of nicotinic acetylcholine receptors that modulate GABA release from CA1 interneurons in rat hippocampal slices. *J Neurosci* **19:**2693–2705.

Alkondon M, Pereira EFR, and Albuquerque EX (2007a) Age-dependent changes in the functional expression of two nicotinic receptor subtypes in CA1 stratum radiatum interneurons in the rat hippocampus. *Biochem Pharmacol* **74:**1134–1144.

Alkondon M, Pereira EFR, Potter MC, Kauffman FC, Schwarcz R, and Albuquerque EX (2007b) Strain-specific nicotinic modulation of glutamatergic transmission in the CA1 field of the rat hippocampus: August Copenhagen Irish versus Sprague-Dawley. *J Neurophysiol* **97:**1163–1170.

Alkondon M, Pereira EFR, Yu P, Arruda EZ, Almeida LE, Guidetti P, Fawcett WP, Sapko MT, Randall WR, Schwarcz R, et al. (2004) Targeted deletion of the kynurenine aminotransferase II gene reveals a critical role of endogenous kynurenic acid in the regulation of synaptic transmission via alpha7 nicotinic receptors in the hippocampus. *J Neurosci* **24:**4635–4648.

Aznavour N, Watkins KC, and Descarries L (2005) Postnatal development of the cholinergic innervation in the dorsal hippocampus of rat: quantitative light and electron microscopic immunocytochemical study. *J Comp Neurol* **486:**61–75.

DeLorenzo RJ, Garnett LK, Towne AR, Waterhouse EJ, Boggs JG, Morton L, Choudhry MA, Barnes T, and Ko D (1999) Comparison of status epilepticus with prolonged seizure episodes lasting from 10 to 29 minutes. *Epilepsia* **40:**164–169.

Fayuk D and Yakel JL (2004) Regulation of nicotinic acetylcholine receptor channel function by acetylcholinesterase inhibitors in rat hippocampal CA1 interneurons. *Mol Pharmacol* **66:**658–666.

Frazier CJ, Rollins YD, Breese CR, Leonard S, Freedman R, and Dunwiddie TV (1998) Acetylcholine activates an α-bungarotoxin-sensitive nicotinic current in rat hippocampal interneurons, but not pyramidal cells. *J Neurosci* **18:**1187–1195.

Freund TF and Buzsáki G (1996) Interneurons of the hippocampus. *Hippocampus* **6:**347–470.

García Peñas JJ, Molins A, and Salas Puig J (2007) Status epilepticus: evidence and controversy. *Neurologist* **13:**S62–S73.

Geneser-Jensen FA (1972) Distribution of acetyl cholinesterase in the hippocampal region of the guinea pig: II. Subiculum and hippocampus. *Z Zellforsch Mikrosk Anat* **124:**546–560.

Institute of Laboratory Animal Resources (1996) *Guide for the Care and Use of Laboratory Animals*, 7th ed, Institute of Laboratory Animal Resources, Commission on Life Sciences, National Research Council, Washington, DC.

Jones S and Yakel JL (1997) Functional nicotinic ACh receptors on interneurons in the rat hippocampus. *J Physiol* **504:**603–610.

Khiroug L, Giniatullin R, Klein RC, Fayuk D, and Yakel JL (2003) Functional mapping and Ca^{2+} regulation of nicotinic acetylcholine receptor channels in rat hippocampal CA1 neurons. *J Neurosci* **23:**9024–9031.

Lintern MC, Wetherell JR, and Smith ME (1998) Differential recovery of acetylcholinesterase in guinea pig muscle and brain regions after soman treatment. *Hum Exp Toxicol* **17:**157–162.

Mann EO and Greenfield SA (2003) Novel modulatory mechanisms revealed by the sustained application of nicotine in the guinea-pig hippocampus in vitro. *J Physiol* **551:**539–550.

McQuiston AR and Madison DV (1999) Nicotinic receptor activation excites distinct subtypes of interneurons in the rat hippocampus. *J Neurosci* **19:**2887–2896.

Newmark J (2007) Nerve agents. *Neurologist* **13:**20–32.

Pereira EFR, Burt DR, Aracava Y, Kan RK, Hamilton TA, Romano JA Jr, Adler M, and Albuquerque EX (2008) Novel medical countermeasure for organophosphorus intoxication: connection to Alzheimer's disease and dementia, in *Chemical Warfare Agents* (Romano JA Jr, Lukey BJ, and Salem H eds) pp 219–232, CRC Press, Boca Raton, FL.

Pereira EFR, Reinhardt-Maelicke S, Schrattenholz A, Maelicke A, and Albuquerque EX (1993) Identification and functional characterization of a new agonist site on nicotinic acetylcholine receptors of cultured hippocampal neurons. *J Pharmacol Exp Ther* **265:**1474–1491.

Santos MD, Alkondon M, Pereira EFR, Aracava Y, Eisenberg HM, Maelicke A, and Albuquerque EX (2002) The nicotinic allosteric potentiating ligand galantamine facilitates synaptic transmission in the mammalian central nervous system. *Mol Pharmacol* **61:**1222–1234.

Schäfer MK, Eiden LE, and Weihe E (1998) Cholinergic neurons and terminal fields revealed by immunohistochemistry for the vesicular acetylcholine transporter. II. The peripheral nervous system. *Neuroscience* **84:**361–376.

Schrattenholz A, Pereira EF, Roth U, Weber KH, Albuquerque EX, and Maelicke A (1996) Agonist responses of neuronal nicotinic acetylcholine receptors are potentiated by a novel class of allosterically acting ligands. *Mol Pharmacol* **49:**1–6.

Schuh RA, Lein PJ, Beckles RA, and Jett DA (2002) Noncholinesterase mechanisms of chlorpyrifos neurotoxicity: altered phosphorylation of Ca^{2+}/cAMP response element binding protein in cultured neurons. *Toxicol Appl Pharmacol* **182:**176–185.

Silveira CL, Eldefrawi AT, and Eldefrawi ME (1990) Putative M2 muscarinic receptors of rat heart have high affinity for organophosphorus anticholinesterases. *Toxicol Appl Pharmacol* **103:**474–481.

Stief F, Zuschratter W, Hartmann K, Schmitz D, and Draguhn A (2007) Enhanced synaptic excitation-inhibition ratio in hippocampal interneurons of rats with temporal lobe epilepsy. *Eur J Neurosci* **25:**519–528.

Wanaverbecq N, Semyanov A, Pavlov I, Walker MC, and Kullmann DM (2007) Cholinergic axons modulate GABAergic signaling among hippocampal interneurons via postsynaptic α7 nicotinic receptors. *J Neurosci* **27:**5683–5693.

Address correspondence to: Dr. Edson X. Albuquerque, Department of Pharmacology and Experimental Therapeutics, University of Maryland School of Medicine, 655 W. Baltimore St., Baltimore, MD 21201. E-mail: ealbuque@umaryland.edu